HHS Public Access

Author manuscript

Nanomedicine. Author manuscript; available in PMC 2020 October 01.

Published in final edited form as:

Nanomedicine. 2019 October ; 21: 102046. doi:10.1016/j.nano.2019.102046.

Interaction of Blood Plasma Proteins with Superhemophobic Titania Nanotube Surfaces

Roberta Maia Sabino[1], **Kirsten Kauk**[2], **Sanli Movafaghi**[3], **Arun Kota**[1,2,3], **Ketul C. Popat**[1,2,3,*]

[1.]School of Advanced Materials Discovery, Colorado State University

[2.]School of Biomedical Engineering, Colorado State University

[3.]Department of Mechanical Engineering, Colorado State University

Abstract

The need to improve blood biocompatibility of medical devices is urgent. As soon as blood encounters a biomaterial implant, proteins adsorb on its surfaces, often leading to several complications such as thrombosis and failure of the device. Therefore, controlling protein adsorption plays a major role in developing hemocompatible materials. In this study, the interaction of key blood plasma proteins with superhemophobic titania nanotube substrates and the blood clotting responses was investigated. The substrate stability was evaluated and fibrinogen adsorption and thrombin formation from plasma were assessed using ELISA. Whole blood clotting kinetics was also investigated, and Factor XII activation on the substrates was characterized by an in vitro plasma coagulation time assay. The results show that superhemophobic titania nanotubes are stable and considerably decrease surface protein adsorption/Factor XII activation as well as delay the whole blood clotting, thus can be a promising approach for designing blood contacting medical devices.

Graphical abstract – short description

In order to reduce the biomaterial interaction with blood, superhemophobic substrates (i.e. surfaces that repel blood) were fabricated by first changing the topography via making nanotubes and then altering the surface chemistry. It was shown that these surfaces reduce protein adsorption and Factor XII activation, thus preventing blood from clotting and being a promising approach to enhance hemocompatibility of biomaterials.

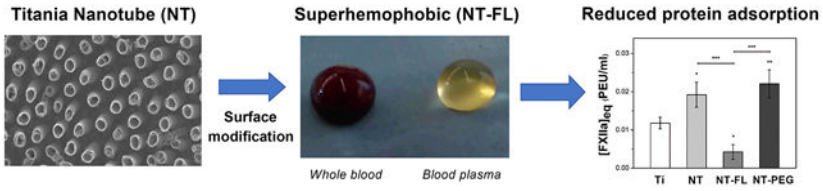

*Author of Correspondence Prof. Ketul C. Popat, ketul.popat@colostate.edu.

Keywords

Protein adsorption; superhemophobic; titania nanotubes; hemocompatibility; factor XII; fibrinogen

Background

Hemocompatibility of biomaterials remains a considerable challenge for successful development of blood-contacting medical devices such as vascular grafts, heart valves, and stents [1]. When biomaterial implants come in contact with blood, the first event is the adsorption of plasma proteins, which can trigger a cascade of mechanisms that cause thrombosis and sometimes failure of the device [2]. A plentiful protein in blood plasma is fibrinogen, and it is one of the first to adsorb on the implant surface when in contact with blood [3]. Fibrinogen is primarily responsible for platelet adhesion, thus being a key protein in the context of the coagulation cascade [4]. This coagulation cascade is a complex process, which can be separated into two distinct pathways: intrinsic and extrinsic. The intrinsic pathway, also called contact activation, is a surface-mediated event and it is the process responsible for clotting on biomaterial surface. It is initiated by the conversion of the protein Factor XII to its activated form FXIIa [5]. Factor XII, also called Hageman Factor, is a coagulation factor, and its autoactivation occurs upon binding with the surface, presumably due to a conformational change [6], [7]. After FXII activation, several proteins are activated in a chain until thrombin is formed [8]. The thrombin then mediates the fibrinogen conversion into fibrin, which polymerizes to form a fibrin mesh that further forms thrombus [9], [10]. Therefore, the study of the interaction between biomaterial surface and blood plasma proteins is essential to understand the mechanisms that can help address the challenge of hemocompatibility [11].

It is well accepted that biomaterial surface characteristics, such as surface chemistry, morphology, and wettability, directly influence the interaction of biomaterial with the blood [12], [13]. Several techniques of surface modification have been investigated in order to enhance hemocompatibility of biomaterial implants. Surface wettability is a key factor in determining the protein adsorption on biomaterial surfaces. Predominantly, hydrophilic surfaces lead to less protein adsorption than hydrophobic surfaces, since hydrophilic surfaces bind strongly with water molecules which constrain proteins from binding with the substrate [14]. One strategy largely studied is the incorporation of various hydrophilic polymers, such as polyethylene glycol (PEG) on biomaterial surfaces [15]. However, previous works have shown that PEG modified materials perform less well in blood and plasma than in simple protein solutions [16]. Another approach is designing superhydrophobic surfaces (i.e. when water contact angles are greater than 150°), and previous studies have shown they can either increase or decrease protein adsorption on surfaces depending on the surface architecture [17].

It is well established that titanium has great biocompatibility and has been widely used as a biomaterial for orthopedic and cardiovascular applications for decades [18]. However, even titanium-based implants can cause adverse effects when in contact with blood [19]. Therefore, one approach that has been recently developed for enhancing hemocompatibility

is making titanium surfaces superhemophobic (i.e. blood plasma contact angles greater than 150°) [20]. Previous study has shown less platelet adhesion and activation on superhemophobic titania nanotubes arrays [21]; however, it is still unclear what happens to specific blood proteins of the coagulation cascade on this surface. In this work, we have studied the potential hemocompatibility of superhemophobic titania nanotube arrays by investigating in detail the blood clotting responses and the interaction of key blood plasma proteins, such as fibrinogen, thrombin and factor XII, with the substrates. In this study, hemophilic, hemophobic, and superhemophobic titania surfaces were fabricated by combination of surface topography (smooth surface and titania nanotube arrays) and surface chemistry (unmodified, fluorinated [22] and PEGylated [21]). The results show that superhemophobic substrates limit surface protein adsorption and FXII activation, as well as delays the whole blood clotting, thus proving to be a good approach for improving hemocompatibility of biomaterials.

Methods

Fabrication of titania nanotube arrays with different surface modification

Titania nanotube arrays were produced from titanium foil (0.5 mm thick) via anodization process described elsewhere [23]. Unmodified titanium and titania nanotube array surfaces were further modified in two different ways. Prior to surface modification, the substrates were treated with oxygen plasma at 200 V in 10 cm^3/min of oxygen gas for 15 mins.

- The substrates were positioned on a hot plate near a glass slide with 200 μl of (heptadecafluoro-1,1,2,2-tetrahydrodecyl)trichlorosilane (referred to as FL). The glass slide and substrates were covered with a bowl and heated at 120 °C for 1 hr.
- The substrates were placed in a 2 vol% solution of 2-[methoxy(polyethyleneoxy)propyl]trimethoxsilane (referred to as PEG) in ethanol solution for 20 hrs.

Following notation will be used in the manuscript: unmodified titanium surface: Ti; unmodified titania nanotube arrays: NT; substrates modified with FL: Ti-FL and NT-FL; substrates modified with PEG: Ti-PEG and NT-PEG.

Surface characterization of different substrates

The surface morphology of different substrates was characterized using scanning electron microscopy (SEM). Static contact angles were obtained using a Ramé-Hart goniometer. The surface chemistry was identified using X-ray photoelectron spectroscopy (XPS). Further, film thickness of substrates treated with FL and PEG were also calculated from the attenuation of XPS signals using the standard overlayer method [24]. The surface crystalline structure was determined by X-ray diffraction (XRD, Shimadzu).

Stability of different substrates in physiological conditions

The stability of different substrates was characterized by measuring the water contact angles over a 28-day period. The substrates were placed in an incubator (37°C and 5% CO_2) on horizontal shaker (100 rpm) plate for 28 days in phosphate buffer saline (PBS). After 7-day

intervals, the substrates were dried, and the contact angles were measured. Further, XPS was also used in order to determine the surface composition after the 28 days.

Fibrinogen adsorption from platelet rich plasma (PRP) on different substrates

Fibrinogen adsorption from PRP on different substrates was assessed using an enzyme-linked immunoassay (ELISA). Sterilized substrates were then incubated in PRP on a horizontal shaker plate (100 rpm) for 2 hrs at 37 °C and 5% CO_2. The protocol from the manufacturer was followed.

Thrombin anti-thrombin (TAT) complex formation on different substrates

TAT complex formation on different substrates exposed to platelet poor plasma (PPP) was investigated using a human TAT Complex ELISA kit (AssayPro). Sterilized substrates were incubated in PPP on a horizontal shaker plate (100 rpm) for 2 hrs at 37 °C and 5% CO_2. The protocol from the manufacturer was followed.

In vitro plasma coagulation assay

FXII activation on different substrates was characterized by an *in vitro* plasma coagulation time (CT) assay. CT is the time demanded from activation of the intrinsic pathway of the coagulation cascade to the occurrence of a visible clot [25]. All CT measurements were performed in PPP.

Factor XIIa (FXIIa) titration curve—Human coagulation FXIIa (Enzyme Research Laboratories) with activity value of 73 plasma equivalent units per mg (PEU/mg) was used in this study. The method described elsewhere was followed [25]. FXIIa activity was quantified using a titration calibration curve relating [FXIIa]eq, in PEU/ml to the plasma coagulation time. A mathematical model developed in a previous study was fitted to the obtained data of coagulation times related to the amount of exogenous FXIIa added [5]. The equation that relates CT to FXIIa concentration through three adjustable parameters a, b, and c is given by:

$$CT = \frac{a[FXIIa] + b}{[FXIIa] + c}$$

with

$$a = \frac{k_b CT_0}{k_1 + k_b}, \qquad b = \frac{k_b CT_0}{k_1 + k_b} K_G \qquad and \qquad c = \frac{k_b K_G}{k_1 + k_b}$$

where CT_0 is the background coagulation time, k_1 and K_G are the reaction rate constant and Michaelis-like constant, respectively, k_b is the reaction rate constant for the background clot, which means the clot formation under assay conditions but with no addition of FXIIa [5].

The commercial software Origin (OriginLab Corporation, Northampton, MA) was used to get the best-fit solution to experimental titration data (CT vs. exogenous FXIIa concentration).

FXII activation in plasma—To obtain the substrate-induced contact activation, PPP was added to sterilized substrates (23 mm^2) in a 2 ml polystyrene micro-cuvette and CT was measured. The method described elsewhere was followed [25]. The CT was then used to calculate the equivalent FXIIa activity by referencing back to the FXIIa titration curve obtained.

Whole blood clotting kinetics

Sterilized substrates were placed in a 24-well plate in order to investigate whole blood clotting kinetics. Human blood from healthy donors was collected in 3 ml sterile centrifuge tubes without any anti-coagulants. 7 μl of this blood was immediately placed onto the substrates, and the droplet was allowed to clot for up to 30 mins. After 15 mins intervals, the substrates were moved into a different 24-well plate with 500 μl of DI water. The substrates were then gently agitated for 30 secs and left in the DI water for 5 mins to lyse the red blood cells and release free hemoglobin from them. The free hemoglobin absorbance was then measured using a plate reader at a wavelength of 540 nm. The absorbance value is directly proportional to the amount of free hemoglobin in DI water and provides a direct relation to the extent of blood clotting on different substrates [26].

Statistical analysis

SEM, XPS and XRD analysis were done on 2 different samples of each substrate. Contact angle and stability test were done using 3 droplets per sample on 3 different samples of each substrate (n_{min}=9). All protein adsorption experiments were repeat twice with 3 samples of each substrate (n_{min}=6). Whole blood clotting kinetics were reconfirmed on 3 different samples of each substrate. Analysis of variance (ANOVA) and Tukey tests were conducted for the experiment data using software Origin 8.5 at a 5% significance level ($p < 0.05$).

All studies discussed below were performed with at least two healthy donors. To avoid donor-to-donor variability, the results presented are only from one donor. However, similar trends were observed for all the donors, which indicates the reproducibility of the results.

Results

SEM was used to characterize the surface morphology of different substrates. As expected, the images indicate smooth topography for unmodified titanium and uniform vertically oriented nanotubes on anodized surface with a diameter of 147 ± 5 nm. (Figure 1). The results also show no apparent changes in morphology of both substrates after modification with FL and PEG. Further, there was no significant difference in nanotube diameter after surface modification ($p<0.05$), with a diameter of 152 ± 6 nm for NT-FL and 155 ± 7 nm for NT-PEG.

Contact angle goniometry was used to characterize the wettability of different substrates. Static contact angles were measured using blood plasma. When the static contact angle (θ) between the surface and blood droplet is greater than 150°, the surface is designated superhemophobic [21]. The surface is considered as hemophilic when $\theta < 90°$, and as hemophobic if $\theta > 90°$ [27]. Based on the results, NT-FL is superhemophobic, since $\theta =$

167°. The results also indicate that Ti-FL is hemophobic; and Ti, Ti-PEG, NT and NT-PEG are hemophilic (Figure 2).

XPS was used to characterize the surface chemistry of different substrates. Survey spectra show that all the substrates had O1s, Ti2p3/2, and C1s peaks (Figure 3a). The C1s peak was present on NT and Ti due to some residues of carbon already present on the substrates and contamination in the XPS chamber. As expected, the results indicate the F1s peak on both surfaces modified with the fluorinated silane FL. The C1s peak increased for Ti-FL and Ti-PEG as compared to Ti; and NT-FL and NT-PEG as compared to NT; since both silanes contain carbon. Further, the O1s peak increased for both Ti-PEG as compare to Ti; and NT-PEG as compared to NT; due to the characteristic CO groups present in the PEGylated silane.

The surface elemental composition for different substrates was also obtained from XPS survey scans using MultiPak software (Table 1). Ti-FL, Ti-PEG, NT-FL, and NT-PEG show an increase in carbon concentration as well as a decrease in titanium concentration compared to unmodified Ti and NT. The reason for this is the presence of silane on the surface that leads to a decrease in titanium concentration after surface modification. In addition, although PEG has oxygen, the percentage concentration of oxygen on both substrates treated with PEG has decreased because of the significant increase in the percentage of carbon. As expected, a high concentration of fluorine was observed for both surfaces treated with FL.

High resolution C1s scans from XPS also indicate the presence of characteristics CF_2 and CF_3 groups on NT-FL and Ti-FL whereas characteristic CO groups (C-O and O-C=O) on hemophilic surfaces (Figure 3b). The presence of these peaks shows that Ti and NT were successfully modified by FL and PEG silanes.

Additionally, silane thickness on Ti and NT after surface modification with FL and PEG were calculated from the attenuation of XPS signals using the standard overlayer method, which determines the film thickness using the intensities of Ti2p peaks before and after silanization. The electron attenuation length for Ti, L_{Ti}, found in the literature is 2.1 nm [28]. Using the intensity of Ti2p peaks from XPS survey spectra of substrates before and after surface modification, the thickness of Ti-FL calculated is 1.83 nm, 0.158 nm for Ti-PEG, 1.04 nm for NT-FL calculated and for NT-PEG the thickness of the film is 0.037 nm.

XRD was used to characterize the surface crystalline structure of different substrates. After the anodization process, the nanotubes are amorphous, and in order to form the crystal phases, annealing process is required. The annealing temperature of 530 °C was chosen to guarantee the total crystallization of titania nanotube arrays [23]. All NT substrates have rutile and anatase crystal phases which are not present on Ti surfaces (Figure 3c). Both anatase and rutile crystal phases provide important characteristics to the material. The rutile phase is the most stable phase, while the metastable anatase phase can produce a more conductive surface and has be shown to be less cytotoxic in TiO_2 crystals [29], [30]. The results also indicate that the surface modification with FL and PEG does not affect the crystalline structure of the unmodified titanium and the titania nanotube arrays.

The stability of different substrates was characterized by measuring the water contact angles every 7 days over a 28-day period. The substrates were placed in an incubator (37°C and 5% CO_2) on a horizontal shaker (100 rpm) for 28 days in PBS, and the contact angles were measured. After this period, the substrates incubated in PBS showed a significant decrease in the contact angles for all Ti groups (Figure 4a), which indicates that these surfaces are not stable under buffer conditions.

XPS was also used to determine the surface composition after 28-day period. The results show a considerable decrease in the CO groups percentage on both samples modified with PEG (Figure 4b), especially for Ti-PEG, which confirm the results obtained with the contact angles. In addition, new CO groups were present on Ti-FL and Ti-PEG. However, the CF2 and CF3 groups are still present with similar amount.

The surface elemental composition for different substrates after 28 days of incubation in PBS was also obtained from XPS survey scans using MultiPak software (Table 2). The results show that Ti-FL and Ti-PEG had a considerable change in their surface composition when compared with day 0 (Table 1). Both groups showed a substantial increase in the percentage of titanium (approximately 100%) and a considerable decrease in carbon concentration (approximately 25%); and Ti-FL also showed a 30% reduction in fluorine concentration. In addition, NT-FL and NT-PEG show very similar elemental composition after 28 days of incubation in PBS, which also suggest their stability under buffer conditions.

Based on the stability results, further studies were not done on Ti-FL and Ti-PEG, since they were not stable under buffer conditions after the 28-day period.

Fibrinogen adsorption from PRP on different substrates was measured using an enzyme-linked immunoassay (ELISA). The PRP was assayed to determine the amount of fibrinogen that remained after exposure to substrates, and this was compared with amount of fibrinogen in PRP that was not exposed to substrates. The results indicate that NT, NT-FL, and NT-PEG had significant lower fibrinogen binding from PRP in comparison with Ti, although no statistically significant difference was observed between NT and NT-FL, and between NT-FL and NT-PEG (Figure 5). The results also show that NT-PEG had significant higher fibrinogen adsorption than NT.

TAT complex formation on different substrates exposed to PPP was investigated using a human TAT Complex ELISA kit. In order to evaluate TAT formation from blood plasma, the substrates were incubated in PPP for 2 hrs, and PPP was then assayed to determine the amount of TAT presenting in plasma. The results show no statistically significant differences in TAT formation between all substrates, although trends indicate that NT-FL and NT-PEG had lower TAT concentrations (Figure 6).

FXII activation on different substrates was characterized by an *in vitro* plasma coagulation time (CT) assay. Previous work has developed a mathematical model that relate CT to FXIIa concentration, through three adjustable parameters *a*, *b*, and *c* [5]. Results of FXIIa titration in PPP show that CT decreases as exogenous FXIIa concentration increases (Figure 7a). The

least squares fitting solution to experimental titration data was obtained using the software Origin. The results for the best fit solution (R=0.947) are given in Table 3.

Contact activation of FXII in plasma by different substrates was measured using a CT assay. The titration curve obtained was used to convert the CT obtained into FXIIa concentration. The results indicate that NT-FL had significant lower FXII activation in plasma in comparison with the other substrates (Figure 7b). Specifically, NT-FL shows an impressive 300% reduction of FXII activation in comparison with Ti and 400% comparing with NT and NT-PEG.

Whole blood clotting kinetics were investigated by measuring the amount of free hemoglobin on different substrates in terms of absorbance. Whole human blood was allowed to clot for 15 and 30 mins on different substrates. The values of free hemoglobin concentration were measured for different substrates after 15 and 30 mins. After this time, the measurements were stopped since the blood starts to clot with the contact with air, which would interfere in the results. The results indicate that blood clotting was significantly delayed on NT-FL substrate in comparison with the other groups (Figure 8). After 30 mins, the amount of free hemoglobin on NT-FL is the same as after 15 mins, and both are close to the un-clotted blood (the absorbance was reduced by 17%). After 30 mins, Ti showed a reduction in the absorbance of 80 %; 45 % for NT and 65 % reduction for NT-PEG.

Discussion

Until now, there is no biomaterial that is completely compatible with blood. Thousands of patients have suffered complications due to blood clotting, and many of them must take blood-thinning medications for years after receiving blood contacting devices [20]. Therefore, there is an urgent need to develop novel materials that prevent blood clotting, and it is essential to understand the initial events that happen on the implant surface when it comes in contact with blood. Immediately after the medical device implantation, blood protein adsorbs on the material surface, which mediates all the subsequent phenomena, such as platelet attachment and thrombus formation [31]. Thus, understanding the way in which proteins interact with the biomaterial surface is fundamental, and the surface characteristics, such as topography and wettability play an important role in the scenario [32]. In this work, we have studied the stability of the substrates and how they interact with key blood proteins from the coagulation cascade, such as fibrinogen, thrombin and Factor XII, as well as the whole blood kinetics.

Titania nanotubes arrays were fabricated by anodizing unmodified titanium sheets in HF solution, and its formation is due to a field-assisted dissolution process [33]. Unmodified titanium and titania nanotube array were then modified with the silanes FL and PEG. Prior to the silanization process, the surfaces were treated with oxygen plasma to form hydroxyl groups. These hydroxyl groups then form covalent bonds with the silanes [34]. In order to make superhemophobic surfaces, the Cassie-Baxter state is preferred [35], and these surfaces can be fabricated by modifying nanotextured surfaces with a low solid surface energy silane [21]. Thus, in this study, we used titania nanotube arrays to provide

nanotexture and were modified by fluorinated FL silane known to possess lower solid surface energy.

Stability plays a central role for medical devices applications, since the biomaterial implant is designed to stay for years, even decades, inside the patient body. The goal was to investigate if superhemophobic substrates are stable for a significant amount of time under physiological conditions. Previous studies have shown that certain types of superhydrophobic surfaces are stable under water if they present sub-micron or smaller scale roughness [36], [37], but nothing was showed under similar body conditions. After the 28-day period, the substrates showed a significant decrease in the contact angles for all Ti groups, which indicates that these surfaces are not stable under buffer conditions (Figure 4a). This can be explained due to the chemical interaction of the PBS salts and the titanium surface. In contrast, all NT substrates didn't show any significant difference in the contact angles after this period. XPS results are in agreement with the contact angles. After the incubation, both substrates modified with PEG showed a great decrease in the CO groups percentage (Figure 4b), which indicates the silane interaction with hydroxyl groups presents in PBS [38]. For NT-FL, the CF2 and CF3 groups are still present with similar amount, which shows the stability of superhemophobic surfaces over a period of 28 days under physiological conditions.

Fibrinogen adsorption from plasma on different substrates was measured using ELISA. When a blood-contacting medical device is implanted, proteins from blood plasma adhere onto the biomaterial surface within seconds [39]. Protein interaction with surfaces is a complex process, and its adsorption involves hydrogen bonding, van der Waals, and electrostatic interactions. Although some steps in protein adsorption are still unclear, it is known that surface chemistry and topography are key factors that directly affect protein adsorption [40].

Fibrinogen plays a fundamental role in the coagulation cascade and is one of the first blood plasma proteins to adsorb on implant surfaces [1]. When adhered to the biomaterial surface and if Factor XII activates the coagulation cascade, it may cause fibrin polymerization and further leading clot formation. Therefore, fibrinogen is directly related to blood clotting and preventing its adsorption can prevent clot formation.

The results show that NT and NT-FL had significant lower fibrinogen adsorption than Ti and NT-PEG (Figure 5). The decreased fibrinogen adsorption on NT-FL was expected due to the Cassie-Baxter state [21] since it tends to minimize the contact area between the surface and the liquid, thus decreasing the amount of protein adsorbed [41], [42]. However, it was expected that NT had higher adsorption than Ti due to the large surface area of nanotubes that provides more locations for proteins to adsorb [23]. The results obtained could be explained by the "Vroman effect", a phenomenon involving a complex sequence of adsorption and desorption steps [10]. Basically, it is a time-dependent variation in the composition of the adsorbed protein layer, as proteins present at a lower concentration in plasma but with high surface activity displace the proteins with higher concentration but which have lower surface activity [43]. Previous studies have shown that high molecular weight kininogen (HMWK), another plasma protein, plays an important role in the removal

of fibrinogen from the surface and this replacement is more likely to happen on hydrophilic substrates [44], [45]. Therefore, because ELISA assay is performed in plasma, this phenomenon happens and the plasma proteins compete with each other for the same adsorbent surface, lowering fibrinogen adsorption on hydrophilic surfaces such as NT [46].

The protein thrombin is the last enzyme in the coagulation cascade, and it is formed by the activation of prothrombin [47]. Thrombin serves to cleave the fibrinogen into fibrin monomers, which further polymerizes to form the thrombus [48], [49]. Therefore, it is desired the lower thrombin generation as possible on the biomaterial surface. The presence of TAT shows the formation of thrombin and the consumption of antithrombin [50].

This study shows no statistically significant differences in TAT formation between all substrates, although trends indicate that NT-FL had lower TAT concentrations (Figure 6). The lower TAT concentration on NT-FL was expected for the same reason as fibrinogen adsorption, due to the Cassie-Baxter state [21]. However, all substrates showed a small amount of TAT generation, and one of the reasons for no significant differences observed between groups could be the premise that whole blood is necessary for satisfactory thrombin formation [51]. Previous studies have shown that TAT generation was practically negligible in PRP and in PPP while meaningful levels of TAT were noted in whole blood since erythrocytes and leukocytes play an important role in thrombin formation [47], [51], [52]. Therefore, the small amounts of TAT generated on all substrates hinder the detection of significant differences between groups.

Contact activation of FXII in plasma by different substrates was measured using a CT assay. Once in contact with the surface of the implant, the activation of FXII is considered one of the major causes of biomaterial-induced blood coagulation [53]. This enzymatic reaction that converts FXII into FXIIa leads the contact activation and initiate the intrinsic pathway of the blood coagulation cascade [54]. Therefore, the interaction of Factor XII with the implant surface plays a vital role in the hemocompatibility since FXII autoactivation upon binding with the surface lead the coagulation cascade.

Although some studies have shown the differences between FXII activation on hydrophilic and hydrophobic surfaces, nothing was explained about superhemophobic materials [25]. The results indicate that superhemophobic substrates had significant lower FXII activation in plasma in comparison with the other substrates in approximately 300% (Figure 7b). It was expected that NT-FL would also decrease FXII activation since it reduces the surface interaction with blood due to the Cassie-Baxter state. In the Cassie–Baxter state, air bags remain stuck underneath the liquid which prevents the liquid droplet to completely wet the surface [21], [55]. This liquid-air-solid interface dramatically decreases the solid-liquid surface area, thus reducing the total area available for proteins to bind [56]. The results obtained show an enormous decreased in FXII activation on NT-FL and that could be the main reason why superhemophobic materials can effectively prevent clot formation.

The coagulation kinetics is vital for the successful use of long term blood-contacting medical devices [23]. One of the further steps in the coagulation cascade is the development of the fibrin mesh, and this matrix traps the red blood cells, which are mainly constituted by

hemoglobin [57], [58]. Whole blood clotting kinetics were investigated by measuring the amount of free hemoglobin on different substrates. As the blood clots on the surface, the red blood cells are trapped inside the fibrin mesh. When the substrates are transferred into water, only the red blood cells that are free in the blood (i.e. not trapped in the fibrin mesh) get lysed. The exposure to water dramatically changes the pressure around the red blood cells, which lyses them thus releasing hemoglobin. Therefore, the free hemoglobin concentration provides a correlation to the extent of blood clotting, with larger amounts of free hemoglobin indicating less clot formation on the substrates [59]. The absorbance value is directly proportional to the free hemoglobin concentration.

The results indicate that blood clotting was significantly delayed on superhemophobic substrate in comparison with the other groups (Figure 8), which is in accordance with the protein results since lower protein adsorption and less FXII activation are expected to reduce the clotting formation.

In summary, this work investigated the detailed interaction of key blood proteins involved in the coagulation cascade with the substrates and their whole blood kinetics. The results could give a better understanding of how blood interact with the implant surface and show that superhemophobic titania nanotubes decrease fibrinogen adsorption as well as tremendously reduce Factor XII. In addition, these surfaces are stable under buffer conditions and considerably delay whole blood clotting, thus showing to greatly enhance hemocompatibility of biomaterials. Future work is now directed towards understanding how cells respond to these substrates.

Supplementary Material

Refer to Web version on PubMed Central for supplementary material.

Acknowledgements

Research reported in this publication was supported by National Heart, Lung and Blood Institute of the National Institutes of Health under award number R01HL135505 and R21HL139208. We also thank the donors of the American Chemical Society Petroleum Research Fund for partial support of this research. The authors acknowledge Patrick McCurdy from CIF CSU for his help with SEM and XPS and Luciane Santos from PUCPR, Brazil for her assistance with XRD.

References

[1]. Jaffer IH, Fredenburgh JC, Hirsh J, Weitz JI. Medical device-induced thrombosis: what causes it and how can we prevent it? J Thromb Haemost 2015; 13:S72–81. doi: 10.1111/jth.12961. [PubMed: 26149053]

[2]. Xia S, Li J, Zu M, Li J, Liu J, Bai X, et al. Small size fullerenol nanoparticles inhibit thrombosis and blood coagulation through inhibiting activities of thrombin and FXa. Nanomedicine Nanotechnology, Biol Med 2018;14:929–39. doi: 10.1016/J.NANO.2017.12.013.

[3]. Xu L-C, Bauer JW, Siedlecki CA. Proteins, platelets, and blood coagulation at biomaterial interfaces. Colloids Surfaces B Biointerfaces 2014;124:49–68. doi: 10.1016/j.colsurfb.2014.09.040. [PubMed: 25448722]

[4]. Wells LA, Guo H, Emili A, Sefton MV. The profile of adsorbed plasma and serum proteins on methacrylic acid copolymer beads: Effect on complement activation. Biomaterials 2017; 118:74–83. doi: 10.1016/j.biomaterials.2016.11.036. [PubMed: 27940384]

[5]. Guo Z, Bussard KM, Chatterjee K, Miller R, Vogler EA, Siedlecki CA. Mathematical modeling of material-induced blood plasma coagulation. Biomaterials 2006;27:796–806. doi: 10.1016/j.biomaterials.2005.06.021. [PubMed: 16099033]

[6]. Chatterjee K, Guo Z, Vogler EA, Siedlecki CA. Contributions of contact activation pathways of coagulation factor XII in plasma. J Biomed Mater Res - Part A 2009;90:27–34. doi: 10.1002/jbm.a.32076.

[7]. Ekdahl KN, Davoodpour P, Ekstrand-Hammarström B, Fromell K, Hamad OA, Hong J, et al. Contact (kallikrein/kinin) system activation in whole human blood induced by low concentrations of α-Fe2O3 nanoparticles. Nanomedicine Nanotechnology, Biol Med 2018;14:735–44. doi: 10.1016/J.NANO.2017.12.008.

[8]. Basmadjian D, Sefton MV, Baldwin SA. Coagulation on biomaterials in flowing blood: Some theoretical considerations. Biomaterials 1997;18:1511–22. doi:10.1016/S0142-9612(97)80002-6. [PubMed: 9430333]

[9]. Liu X, Yuan L, Li D, Tang Z, Wang Y, Chen G, et al. Materials Chemistry B 2014;2:5709–926.

[10]. De Mel A, Cousins BG, Seifalian AM. Surface modification of biomaterials: A quest for blood compatibility. Int J Biomater 2012;2012. doi:10.1155/2012/707863.

[11]. Tsyganov I, Maitz MF, Wieser E. Blood compatibility of titanium-based coatings prepared by metal plasma immersion ion implantation and deposition. Appl Surf Sci 2004;235:156–63. doi: 10.1016/J.APSUSC.2004.05.134.

[12]. Meder F, Brandes C, Treccani L, Rezwan K. Controlling protein–particle adsorption by surface tailoring colloidal alumina particles with sulfonate groups. Acta Biomater 2013;9:5780–7. doi: 10.1016/J.ACTBIO.2012.11.012. [PubMed: 23164944]

[13]. Fabre H, Mercier D, Galtayries A, Portet D, Delorme N, Bardeau J-F. Impact of hydrophilic and hydrophobic functionalization of flat TiO2/Ti surfaces on proteins adsorption. Appl Surf Sci 2018;432:15–21. doi:10.1016/J.APSUSC.2017.08.138.

[14]. Xu LC, Bauer JW, Siedlecki CA. Proteins, platelets, and blood coagulation at biomaterial interfaces. Colloids Surfaces B Biointerfaces 2014;124:49–68. doi: 10.1016/j.colsurfb.2014.09.040. [PubMed: 25448722]

[15]. Kovach KM, Capadona JR, Sen Gupta A, Potkay JA. The effects of PEG-based surface modification of PDMS microchannels on long-term hemocompatibility. J Biomed Mater Res Part A 2014;102A:4195–4205. doi:10.1002/jbm.a.35090.

[16]. Liu X, Yuan L, Li D, Tang Z, Wang Y, Chen G, et al. Blood compatible materials: state of the art. J Mater Chem B 2014;2:5718–38. doi:10.1039/C4TB00881B.

[17]. Song W, Mano JF. Interactions between cells or proteins and surfaces exhibiting extreme wettabilities. Soft Matter 2013;9:2985. doi:10.1039/c3sm27739a.

[18]. Adell R, Lekholm U, Rockler B, Brånemark P-I. A 15-year study of osseointegrated implants in the treatment of the edentulous jaw. Int J Oral Surg 1981;10:387–416. doi: 10.1016/S0300-9785(81)80077-4. [PubMed: 6809663]

[19]. Huang N, Yang P, Leng YX, Chen JY, Sun H, Wang J, et al. Hemocompatibility of titanium oxide films. Biomaterials 2003;24:2177–87. doi:10.1016/S0142-9612(03)00046-2. [PubMed: 12699653]

[20]. Bartlet K, Movafaghi S, Kota A, Popat KC. Superhemophobic titania nanotube array surfaces for blood contacting medical devices. RSC Adv 2017;7:35466–76. doi: 10.1039/C7RA03373G.

[21]. Movafaghi S, Leszczak V, Wang W, Sorkin JA, Dasi LP, Popat KC, et al. Hemocompatibility of Superhemophobic Titania Surfaces". Adv Healthc Mater 2017. doi: 10.1002/adhm.201700647.

[22]. Gao L, McCarthy TJ. How Wenzel and Cassie were wrong. Langmuir 2007;23:3762–5. doi: 10.1021/la062634a. [PubMed: 17315893]

[23]. Smith BS, Yoriya S, Grissom L, Grimes CA, Popat KC. Hemocompatibility of titania nanotube arrays. J Biomed Mater Res - Part A 2010;95 A:350–60. doi: 10.1002/jbm.a.32853.

[24]. Popat KC, Mor G, Grimes CA, Desai TA. Surface modification of nanoporous alumina surfaces with poly(ethylene glycol). Langmuir 2004;20:8035–41. doi:10.1021/la049075x. [PubMed: 15350069]

[25]. Bauer JW, Xu L-C, Vogler EA, Siedlecki CA. Surface dependent contact activation of factor XII and blood plasma coagulation induced by mixed thiol surfaces. Biointerphases 2017;12:02D410. doi: 10.1116/1.4983634.

[26]. Damodaran VB, Leszczak V, Wold KA, Lantvit SM, Popat KC, Reynolds MM. Antithrombogenic properties of a nitric oxide-releasing dextran derivative: evaluation of platelet activation and whole blood clotting kinetics n.d. doi:10.1039/c3ra45521a.

[27]. Wang W, Lockwood K, Boyd LM, Davidson MD, Movafaghi S, Vahabi H, et al. Superhydrophobic Coatings with Edible Materials. ACS Appl Mater Interfaces 2016;8:18664–8. doi: 10.1021/acsami.6b06958. [PubMed: 27403590]

[28]. Pouilleau J, Devilliers D, Garrido F, Durand-Vidal S, Mahé E. Structure and composition of passive titanium oxide films. Mater Sci Eng B 1997;47:235–43. doi:10.1016/S0921-5107(97)00043-3.

[29]. Sorkin JA, Hughes S, Soares P, Popat KC. Titania nanotube arrays as interfaces for neural prostheses. Mater Sci Eng C 2015;49:735–45. doi:10.1016/J.MSEC.2015.01.077.

[30]. Zhang D, Li G, Wang H, Ming Chan K, Yu JC. Biocompatible Anatase Single-Crystal Photocatalysts with Tunable Percentage of Reactive Facets 2010;10:1130–7. doi: 10.1021/cg900961k.

[31]. Huang Y, Lü X, Qian W, Tang Z, Zhong Y. Competitive protein adsorption on biomaterial surface studied with reflectometric interference spectroscopy. Acta Biomater 2010;6:2083–90. doi: 10.1016/J.ACTBIO.2009.12.035. [PubMed: 20026435]

[32]. Lin W, Zhang J, Wang Z, Chen S. Development of robust biocompatible silicone with high resistance to protein adsorption and bacterial adhesion. Acta Biomater 2011;7:2053–9. doi: 10.1016/J.ACTBIO.2011.02.001. [PubMed: 21300187]

[33]. Mor GK, Varghese OK, Paulose M, Mukherjee N, Grimes CA. Fabrication of tapered, conical-shaped titania nanotubes. J Mater Res 2003;18:2588–93. doi: 10.1557/JMR.2003.0362.

[34]. Blitz JP, Little CB. Fundamental and applied aspects of chemically modified surfaces. n.d.

[35]. Movafaghi S, Wang W, Metzger A, Williams DD, Williams JD, Kota AK. Tunable superomniphobic surfaces for sorting droplets by surface tension. Lab Chip 2016;16:3204–9. doi: 10.1039/C6LC00673F. [PubMed: 27412084]

[36]. Xu M, Sun G, Kim C-J. Infinite Lifetime of Underwater Superhydrophobic States. Phys Rev Lett 2014; 113:136103. doi: 10.1103/PhysRevLett.113.136103. [PubMed: 25302907]

[37]. Jones PR, Hao X, Cruz-Chu ER, Rykaczewski K, Nandy K, Schutzius TM, et al. Sustaining dry surfaces under water. Sci Rep 2015;5:12311. doi:10.1038/srep12311. [PubMed: 26282732]

[38]. Puleo DA. Retention of enzymatic activity immobilized on silanized Co-Cr-Mo and Ti-6A1-4V. J Biomed Mater Res 1997;37:222–8. doi: 10.1002/(SICI)1097-4636(199711)37:2<222::AID-JBM11>3.0.CO;2-G. [PubMed: 9358315]

[39]. Leszczak V, Smith BS, Popat KC. Hemocompatibility of polymeric nanostructured surfaces. J Biomater Sci Polym Ed 2013;24:1529–48. doi: 10.1080/09205063.2013.777228. [PubMed: 23848447]

[40]. Roach P, Farrar D, Perry CC. Interpretation of protein adsorption: Surface-induced conformational changes. J Am Chem Soc 2005;127:8168–73. doi:10.1021/ja042898o. [PubMed: 15926845]

[41]. Sun T, Tan H, Han D, Fu Q, Jiang L. No platelet can adhere-largely improved blood compatibility on nanostructured superhydrophobic surfaces. Small 2005;1:959–63. doi: 10.1002/smll.200500095. [PubMed: 17193377]

[42]. Pendurthi A, Movafaghi S, Wang W, Shadman S, Yalin AP, Kota AK. Fabrication of Nanostructured Omniphobic and Superomniphobic Surfaces with Inexpensive CO 2 Laser Engraver 2017. doi:10.1021/acsami.7b06924.

[43]. Nath N, Hyun J, Ma H, Chilkoti A. Surface engineering strategies for control of protein and cell interactions. Surf Sci 2004;570:98–110. doi:10.1016/J.SUSC.2004.06.182.

[44]. Elwing H, Askendal A, Lundström I. Competition between adsorbed fibrinogen and high-molecular-weight kininogen on solid surfaces incubated in human plasma (the vroman effect): Influence of solid surface wettability. J Biomed Mater Res 1987;21:1023–8. doi: 10.1002/jbm.820210808. [PubMed: 3654686]

[45]. Schmaier AH, Silver L, Adams AL, Fischer GC, Munoz PC, Vroman L, et al. The Effect Of High Molecular Weight Kininogen On Surface-adsorbed Fibrinogen. Thromb Reserach 1983;33:51–67.

[46]. Noh H, Vogler EA. Volumetric interpretation of protein adsorption: Competition from mixtures and the Vroman effect. Biomaterials 2007;28:405–22. doi: 10.1016/j.biomaterials.2006.09.006. [PubMed: 17007920]

[47]. Gorbet MB, Sefton MV. Biomaterial-associated thrombosis: Roles of coagulation factors, complement, platelets and leukocytes. Biomater Silver Jubil Compend 2006;25:219–41. doi: 10.1016/B978-008045154-1.50025-3.

[48]. Sperling C, Fischer M, Maitz MF, Werner C. Blood coagulation on biomaterials requires the combination of distinct activation processes. Biomaterials 2009;30:4447–56. doi: 10.1016/J.BIOMATERIALS.2009.05.044. [PubMed: 19535136]

[49]. Colman RW, Schmaier AH. Contact system: a vascular biology modulator with anticoagulant, profibrinolytic, antiadhesive, and proinflammatory attributes. Blood 1997;90:3819–43. [PubMed: 9354649]

[50]. Johnell M, Larsson R, Siegbahn A. The influence of different heparin surface concentrations and antithrombin-binding capacity on inflammation and coagulation. Biomaterials 2005;26:1731–9. doi: 10.1016/j.biomaterials.2004.05.029. [PubMed: 15576147]

[51]. Thor A, Rasmusson L, Wennerberg A, Thomsen P, Hirsch J-M, Nilsson B, et al. The role of whole blood in thrombin generation in contact with various titanium surfaces. Biomaterials 2007;28:966–74. doi: 10.1016/J.BIOMATERIALS.2006.10.020. [PubMed: 17095084]

[52]. Hong Jaan, Ekdahl Kristina Nilsson, Reynolds Helena, Rolf Larsson BN. A new in vitro model to study interaction between whole blood and biomaterials. Studies of platelet and coagulation activation and the effect of aspirin. Biomaterials 1999;20:603–11. [PubMed: 10208402]

[53]. Zhuo R, Siedlecki CA, Vogler EA. Autoactivation of blood factor XII at hydrophilic and hydrophobic surfaces. Biomaterials 2006;27:4325–32. doi: 10.1016/J.BIOMATERIALS.2006.04.001. [PubMed: 16644008]

[54]. Xu L-C, Meyerhoff ME, Siedlecki CA. Blood coagulation response and bacterial adhesion to biomimetic polyurethane biomaterials prepared with surface texturing and nitric oxide release. Acta Biomater 2019;84:77–87. doi: 10.1016/J.ACTBIO.2018.11.035. [PubMed: 30471478]

[55]. Patankar NA. On the Modeling of Hydrophobic Contact Angles on Rough Surfaces 2003. doi: 10.1021/la026612.

[56]. Falde EJ, Yohe ST, Colson YL, Grinstaff MW. Superhydrophobic materials for biomedical applications. Biomaterials 2016;104:87–103. doi: 10.1016/J.BIOMATERIALS.2016.06.050. [PubMed: 27449946]

[57]. Damodaran VB, Leszczak V, Wold KA, Lantvit SM, Popat KC, Reynolds MM. Antithrombogenic properties of a nitric oxide-releasing dextran derivative: Evaluation of platelet activation and whole blood clotting kinetics. RSC Adv 2013;3:24406–14. doi: 10.1039/c3ra45521a.

[58]. Stadler AM, Digel I, Artmann GM, Embs JP, Zaccai G, Büldt G. Hemoglobin dynamics in red blood cells: correlation to body temperature. Biophys J 2008;95:5449–61. doi: 10.1529/biophysj.108.138040. [PubMed: 18708462]

[59]. Simon-Walker R, Cavicchia J, Prawel DA, Dasi LP, James SP, Popat KC. Hemocompatibility of hyaluronan enhanced linear low density polyethylene for blood contacting applications. J Biomed Mater Res - Part B Appl Biomater 2017:1–12. doi: 10.1002/jbm.b.34010.

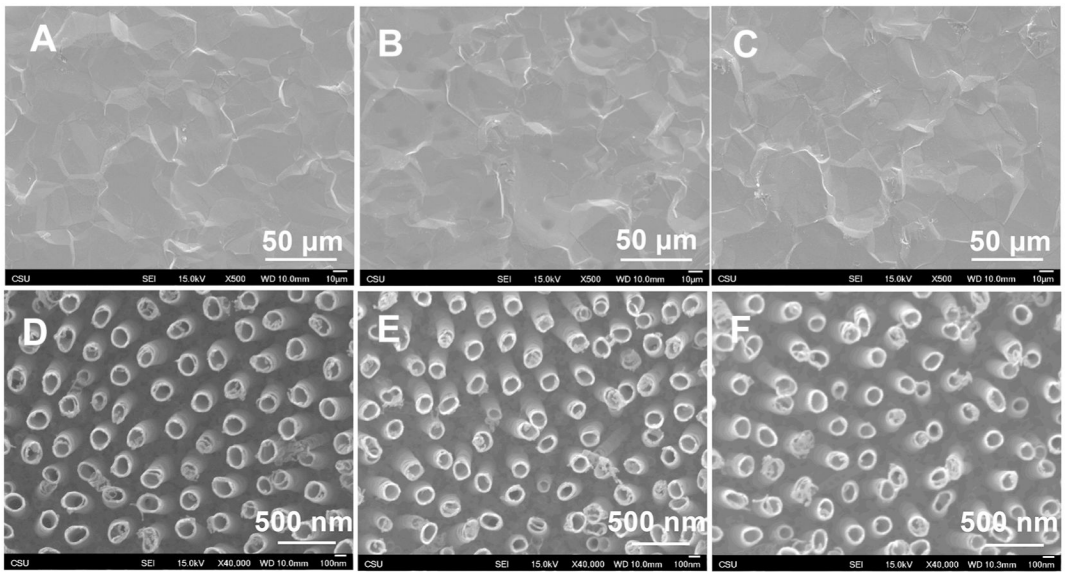

Figure 1.
SEM images for (a) Ti, (b) Ti-FL, (c) Ti-PEG, (d) NT (e) NT-FL and (f) NT-PEG.

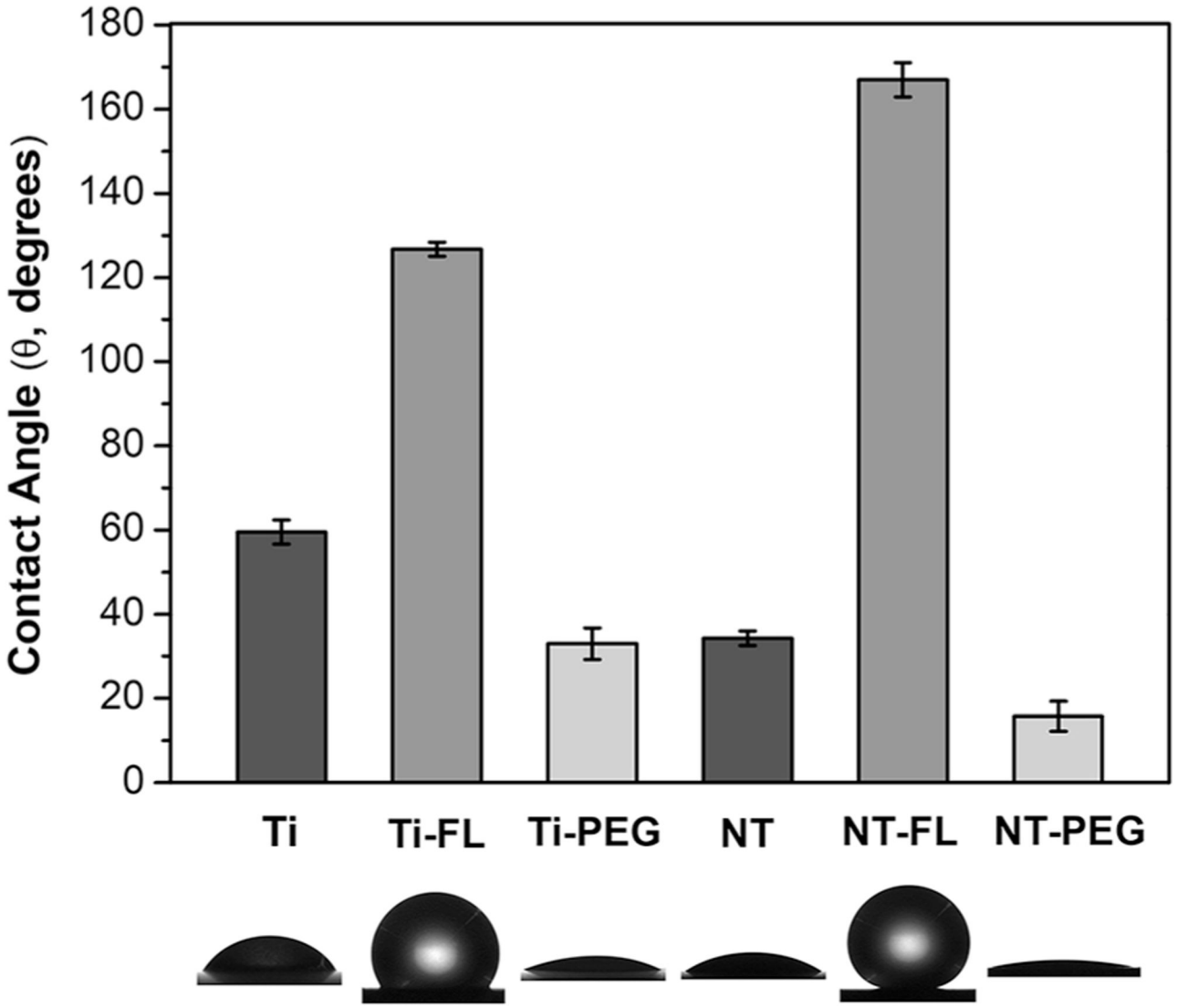

Figure 2.

Static contact angles of human blood plasma for different substrates. No significant differences in contact angle on Ti-PEG and NT. Significant differences in contact angles for all other substrates ($p<0.05$).

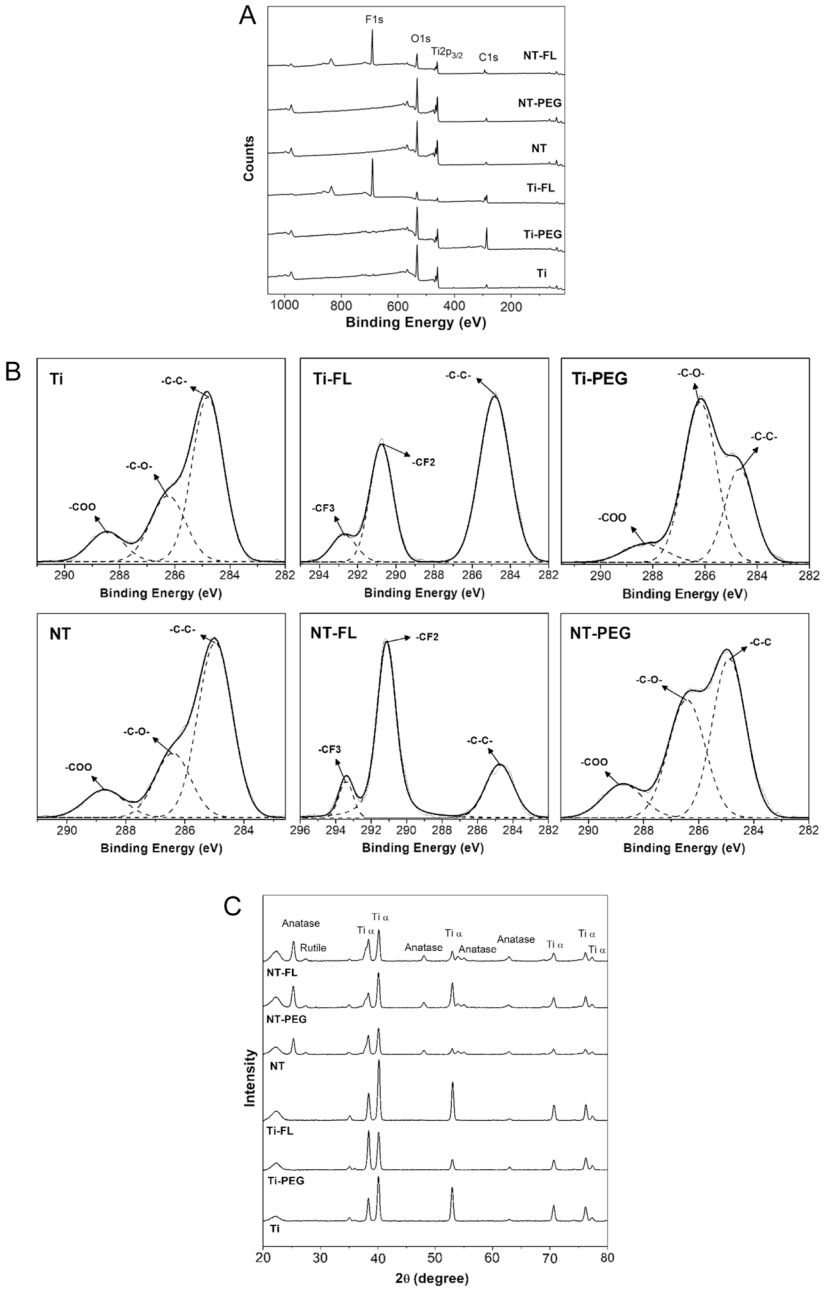

Figure 3.

a XPS survey scans for different substrates.

b High resolution C1s scans for different substrates.

c XRD scans for different substrates.

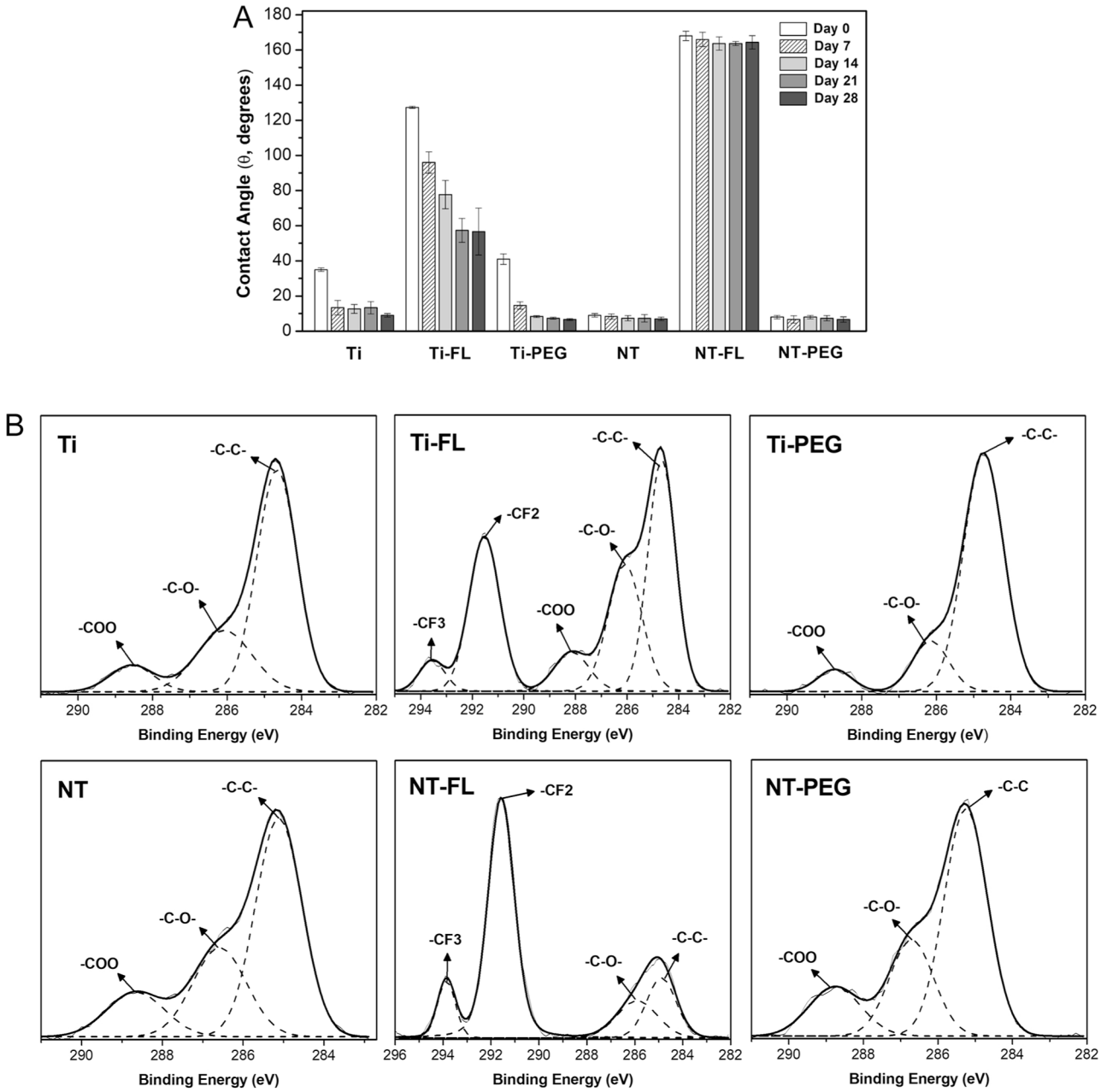

Figure 4.

a Static contact angles for different substrates after 0, 7, 14, 21, and 28 days of incubation.

b High resolution C1s scans for different substrates after 28 days of incubation.

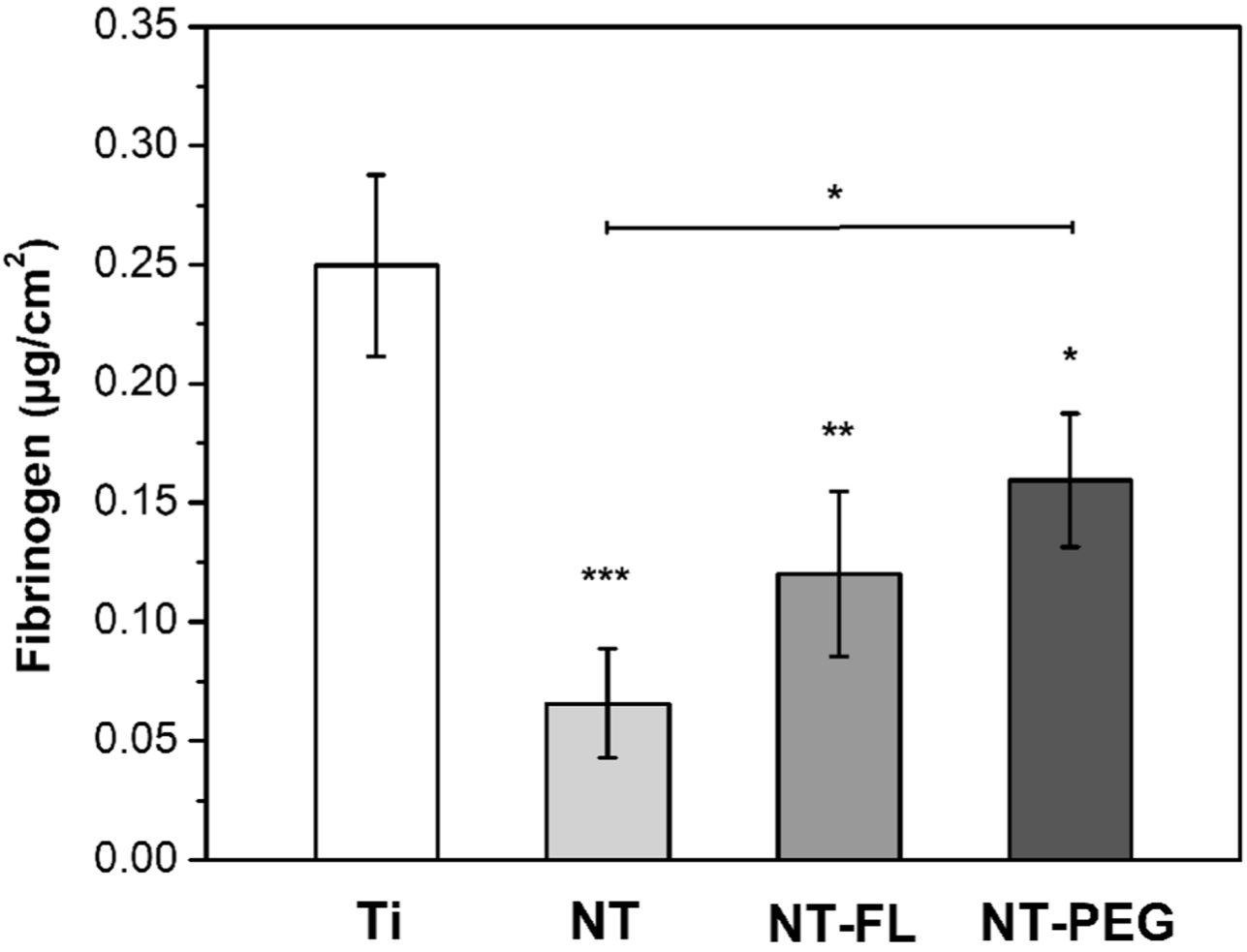

Figure 5.
Fibrinogen binding from PRP on different substrates.

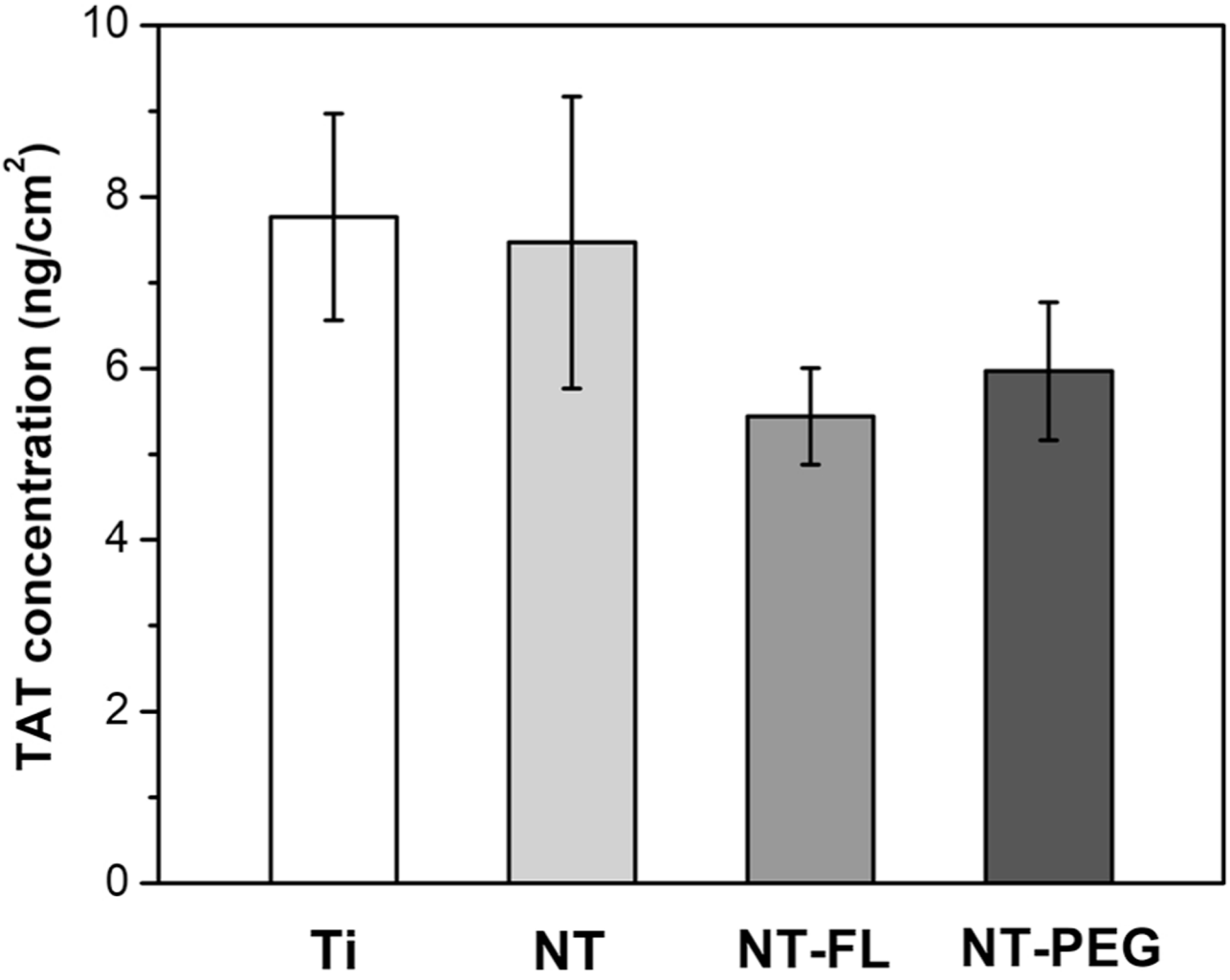

Figure 6.
TAT generation on different substrates after 2 hrs of incubation in PPP. No significant difference between groups was observed ($p<0.05$).

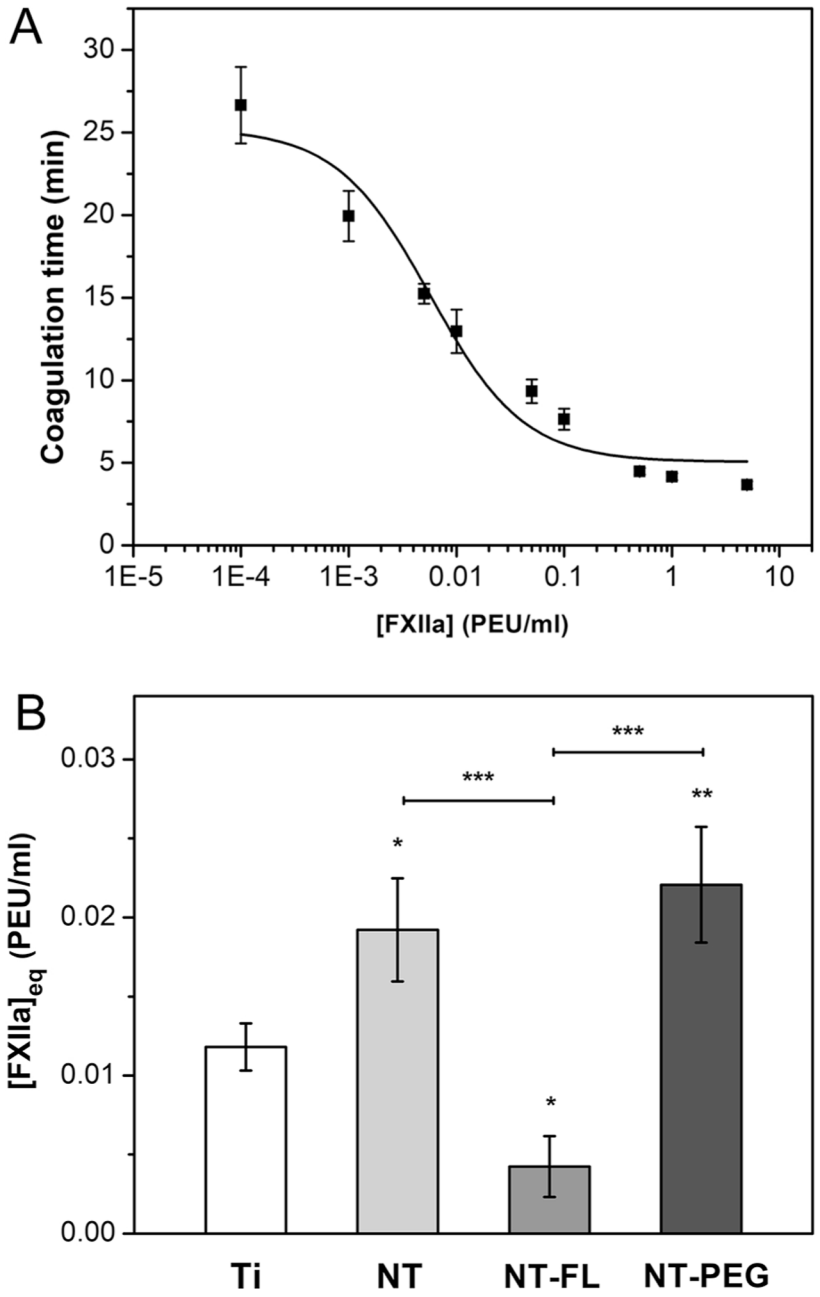

Figure 7.

a FXIIa titration curve for the plasma showing coagulation times versus concentrations of exogenous FXIIa. The fitted curve corresponds to a least squares fitting of a developed mathematical model [5].

b [FXIIa]eq in plasma calculated from coagulation times of different substrates. Ti is used as control for the statistical analysis ($p<0.05$).

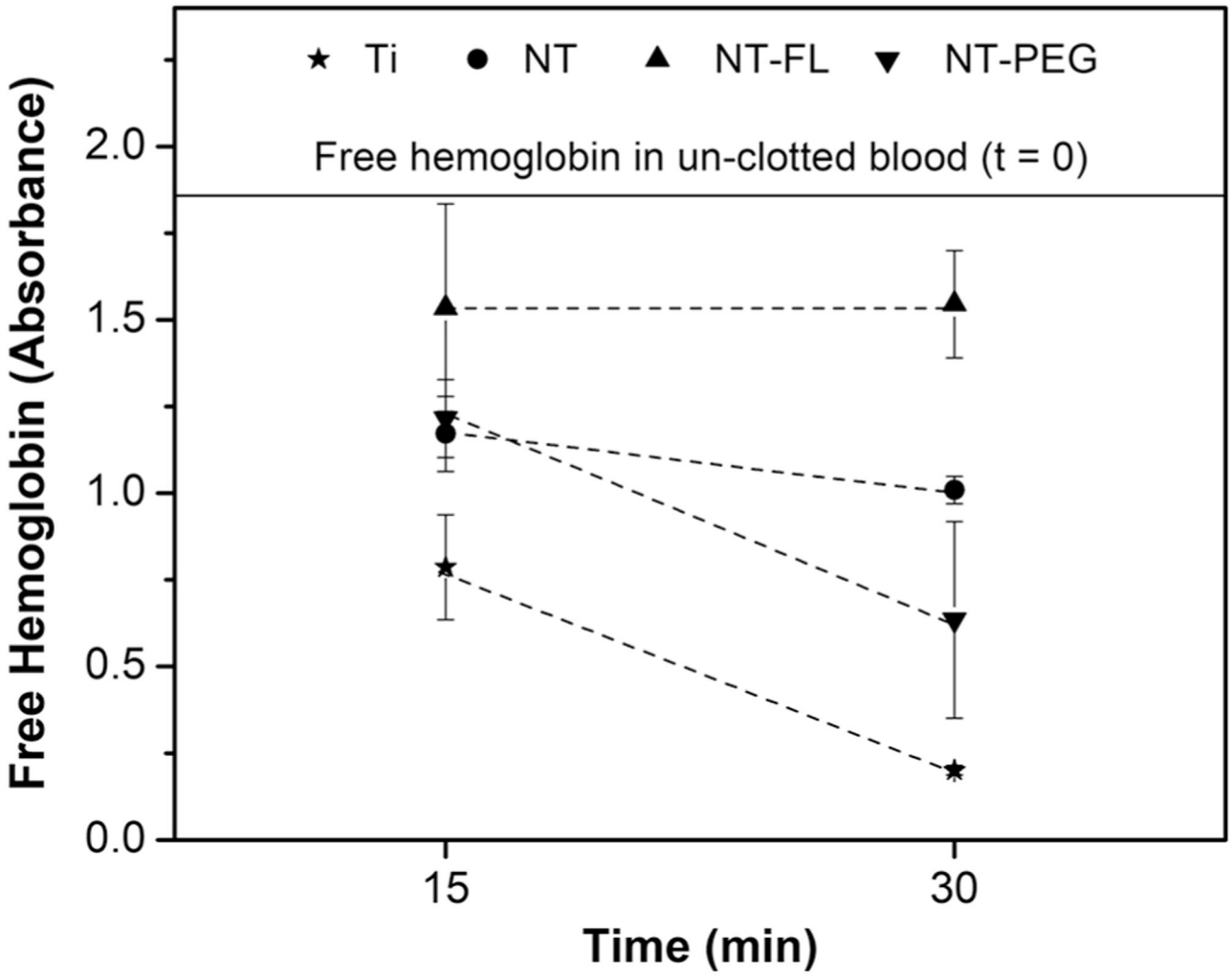

Figure 8.
Free hemoglobin concentration values measured in terms of absorbance for different substrates.

Table 1:

XPS Elemental composition for different substrates.

	% O	% TI	% C	% F
Ti	68.4	13.1	18.5	0
Ti-FL	13.5	1.8	40.5	44.2
Ti-PEG	38.8	7.8	53.4	0
NT	68.3	20.0	11.7	0
NT-FL	21.9	5.3	21.2	51.6
NT-PEG	62.2	17.6	20.2	0

Table 2:

XPS Elemental composition for different substrates after 28 days of incubation in PBS at 37° and 100 rpm.

	% O	% TI	% C	% F
Ti	63.8	10.7	25.5	0
Ti-FL	33.4	5.3	31.8	29.4
Ti-PEG	62.9	11.3	25.8	0
NT	64.3	17.0	18.7	0
NT-FL	26.3	7.0	19.6	47.2
NT-PEG	63.6	16.6	19.9	0

Table 3:

Parameters derived from best fit solution of FXIIa titration data.

	A	B	C
	(5.05 ± 0.91)	(0.14 ± 0.04)	$(5.7 + 2.0) \times 10^{-3}$
Unit	min	μM min	μM